




Article

# Superhydrophobic Bio-Coating Made by Co-Continuous Electrospinning and Electrospaying on Polyethylene Terephthalate Films Proposed as Easy Emptying Transparent Food Packaging

Maria Pardo-Figuerez <sup>1,2</sup>, Alex López-Córdoba <sup>3,4</sup> , Sergio Torres-Giner <sup>1</sup>  and José M. Lagaron <sup>1,\*</sup> 

<sup>1</sup> Novel Materials and Nanotechnology Group, Institute of Agrochemistry and Food Technology (IATA), Spanish National Research Council (CSIC), Calle Catedrático Agustín Escardino Benlloch 7, 46980 Paterna, Valencia, Spain; mpardo@iata.csic.es (M.P.-F.); storresginer@iata.csic.es (S.T.-G.)

<sup>2</sup> Bioinicia R&D Department, Bioinicia S.L. Calle Algepser 65, nave 3, 46980 Paterna, Valencia, Spain

<sup>3</sup> Laboratorio de Polímeros y Materiales Compuestos (LP&MC), Instituto de Física de Buenos Aires (IFIBA-CONICET), Departamento de Física, Facultad de Ciencias Exactas y Naturales, Universidad de Buenos Aires, Buenos Aires C1428EGA, Argentina; alexlcordova@gmail.com

<sup>4</sup> Escuela de Administración de Empresas Agropecuarias, Facultad Seccional Duitama, Universidad Pedagógica y Tecnológica de Colombia, Carrera 18 con Calle 22, Duitama 150461, Boyacá, Colombia

\* Correspondence: lagaron@iata.csic.es; Tel.: +34-963-900-022

Received: 17 September 2018; Accepted: 11 October 2018; Published: 16 October 2018



**Abstract:** Interest in coated films with micro/nanofeatures has grown rapidly in recent years due to their enhanced functional performance and better durability under demanding contact conditions or aggressive environments. In the current work, it is reported a one-step co-continuous bilayer coating process to generate a multilayer film that rendered superhydrophobicity to a polyethylene terephthalate (PET) substrate. A continuous coating based on ultrathin polylactide (PLA) fibers was deposited onto PET films by means of electrospinning, which increased the water contact angle of the substrate. Sequentially, nanostructured silica (SiO<sub>2</sub>) microparticles were electrospayed onto the coated PET/PLA films to achieve superhydrophobic behavior. This multilayer was then treated at different annealing temperatures, that is, 150 °C, 160 °C, and 170 °C, in order to create interlayers' adhesion to each other and to the substrate. It was found that co-continuous deposition of PLA fibers and nanostructured SiO<sub>2</sub> microparticles onto PET films constituted a useful strategy to increase the surface hydrophobicity of the PET substrate, achieving an optimal apparent water contact angle of 170° and a sliding angle of 6°. Unfortunately, a reduction in background transparency was observed compared to the uncoated PET film, especially after electrospaying of the SiO<sub>2</sub> microparticles but the films were seen to have a good contact transparency. The materials developed show significant potential in easy emptying transparent food packaging applications.

**Keywords:** electrospinning; electrospaying; superhydrophobicity; polyethylene terephthalate (PET); polylactide (PLA)

## 1. Introduction

Coatings are defined as mixtures of film-forming materials containing solvents and other additives that, when applied to a surface and after curing/drying process, yield a solid, protective, decorative, and/or functional adherent thin layer [1]. Surface coatings include paints, drying oils and varnishes, synthetic clear coatings and other products. Coating on substrates offer several advantages, such

as the fact that coated materials have better durability against demanding contact conditions or aggressive environments than the raw materials [2]. Moreover, coatings allow the enhancement of certain properties that the raw materials could not provide, such as antimicrobial, self-cleaning, superhydrophobic and antifouling effects, and so forth [3–5].

Over the past years, nanotechnology has emerged as a potential tool in the development of surface coatings [2], resulting in their use in fields such as electronics, medical, food, pharmacy and aerospace. These surface coatings can contain micro/nanoscale features that offer more optimal and processing properties than conventional coatings, such as higher opacity, better interaction between the coating and surface and higher durability of the coating [2]. Moreover, coatings containing topographical cues may impart hydrophobic and oleophobic properties, thus improving corrosion resistance and enhancing either insulative or conductive properties [4].

The generation of superhydrophobic coatings has been gaining a fair interest in the field of coating technology [6,7]. Superhydrophobic coatings are specifically referred to water repellent layers with a water contact angle  $>150^\circ$  [8]. Such coatings can be prepared either by fabricating rough architectures on the surface or by chemically modifying rough surfaces containing low surface free energy materials [8,9]. These surfaces can often be accomplished by common techniques such as dip coating [10], lithography [11,12], chemical vapor deposition [13], among others [14]. However, the common processes to obtain such coatings are considered complex and their industrial applications are still limited. Therefore, new developments in coating technology are necessary in order to expand the accessibility of superhydrophobic coatings.

Electrohydrodynamic processing (EHDP), including electrospinning and electrospraying, is a very appealing technology that can be used to apply topographical structured (such as fibers or particles) layers on a wide variety of substrates [15]. These technologies utilize high electrostatic potentials to draw polymer solutions or polymer melts into fibers or particles [16,17]. Electrospinning/electrospraying processes present the advantage to work at atmospheric pressure and are, therefore, easily integrate into continuous production lines. Moreover, unlike vapor deposition, these novel technologies allow the application of a continuous layer with the required surface roughness necessary to exhibit superhydrophobic properties [4]. The structure and the physicochemical properties of the electrospun fibers and electrosprayed particles generated by EHDP can also be tailored according to the end application, for instance packaging [18,19]. Moreover, both techniques enable to process many synthetic and natural polymers either alone or blended with other polymers and/or additives (e.g., surfactants). Among them, polylactide (PLA) is one of the most attractive materials for coating fabrication by electrospinning/electrospraying because it is easily spinnable, biodegradable, and thermoplastic [4,20].

Likewise, functional coatings containing particles of titanium dioxide ( $\text{TiO}_2$ ), silicon dioxide ( $\text{SiO}_2$ , also known as silica), carbon black (CB), iron oxide ( $\text{Fe}_2\text{O}_3$ ), and zinc oxide (ZnO) have been developed [3]. Among them,  $\text{SiO}_2$ -based coatings have been of particular interest as such coatings can offer self-cleaning properties as well as antimicrobial functionality. The use of  $\text{SiO}_2$  microparticles for coating deposition allows for a change on the surface roughness and surface energy, leading to a superhydrophobic behavior without the need to perform any chemical modification [7,9]. As these surfaces are also highly water-repellent, they can be used in mirrors, self-cleaning windows, frames, bricks, wall paint, tiles, flat glass, and so forth [21]. Recently, Lasprilla-Botero et al. [8] reported an interesting approach to the design of superhydrophobic films by means of electrospinning/electrospraying, depositing electrospun ultrathin poly( $\epsilon$ -caprolactone) (PCL) fibers followed by electrosprayed nanostructured silica ( $\text{SiO}_2$ ) microparticles onto low-density polyethylene (LDPE) films. The resultant coated films showed a high surface hydrophobicity with an apparent contact angle of  $157^\circ$ . Moreover, they showed good adhesion between layers and improved thermal stability.

In the current work, a similar but a one-step continuous electrospinning/electrospraying process was applied to generate a superhydrophobic PLA/ $\text{SiO}_2$  bilayer on polyethylene terephthalate (PET)

substrates with the additional aim of achieving maximum transparency. The process consisted of a deposition of PLA fibers and SiO<sub>2</sub> microparticles sequentially onto a PET film by electrospinning and electro spraying, respectively, and a subsequent annealing to improve the adhesion between the layers. To the best of our knowledge, this is the first time that PET films are coated with a PLA/SiO<sub>2</sub> bilayer obtaining not only high superhydrophobicity but also a good adhesion between layers using a scalable one-step continuous process.

## 2. Materials and Methods

### 2.1. Materials

The substrate PET, with a thickness of  $77.0 \pm 0.6 \mu\text{m}$ , was kindly provided from Belectric OPV GmbH (OPVIUS-Organic Photovoltaic Solutions, Kitzingen, Germany). For the films deposition, PLA was an Ingeo™ Biopolymer 2003D with melting features determined by differential scanning calorimetry (DSC) from 145 to 160 °C as reported by the manufacturer, NatureWorks LLC (Minnetonka, MN, USA). The SiO<sub>2</sub> microparticles (HDK® H18, Pyrogenic Silica) were obtained from Wacker Chemie AG (München, Germany). Polyvinylpyrrolidone (PVP), with a molecular weight ( $M_w$ ) of 40,000 g/mol, was provided by Sigma Aldrich S.A. (Madrid, Spain). Chloroform, acetone, and ethanol with purities >99.5% were supplied by Panreac Química S.A. (Barcelona, Spain).

### 2.2. Preparation of Multilayer Films

#### 2.2.1. Solutions

The solution for electrospinning was prepared by dissolving 7.5 wt.% PLA in a chloroform/acetone 7:3 (vol./vol.) solution and further stirring until complete dissolution. For electro spraying, a 1.5 wt.% of SiO<sub>2</sub> microparticles were suspended in ethanol and ultrasonicated for 1–2 min prior to electro spraying. Concentrations were optimized in preliminary experiments based on a previous work [22].

#### 2.2.2. Electrospinning and Electro spraying of PLA Fibers and SiO<sub>2</sub> Microparticles

The tailor-made pilot equipment utilized for the formation of the bilayers consisted of two single needle injectors, one for electrospinning (PLA) and one for electro spraying (SiO<sub>2</sub>), which sequentially deposited fibers and microparticles onto the PET film using an AC controlled proprietary Fluidnatek® LE500 pilot line from Bioinicia S.L. (Valencia, Spain, see Figure 1). The roll containing the PET films was moving over the roll-to-roll system in continuous at a speed of 1 mm/s. Initially, for optimization purposes, the PET films were only coated with an electro spun layer of PLA fibers. To this end, the PET films were first placed on the continuous roll-to-roll collector and the PLA solution was then pumped in one of the injectors at a flow-rate of 20 mL/h through a needle with an inner diameter of 0.8 mm and a distance to the collector of 15 cm. The electrical voltages of the dual polarizers were set at 17 kV and –4 kV using a high-voltage supply unit in which the spinneret filled with the polymer solution was connected to the positive terminal of the power supply and the collector was to the negative electrode (ground). Optimal deposition was found when the collector was placed at a distance of 12 cm. The process was carried out in the air conditioning (AC) system—controlled environmental chamber set at 23 °C and 40% relative humidity (RH).

Once the PLA deposition was optimized (PET/PLA films), the second injector for electro spraying was incorporated into the system to obtain a sequential electro spinning of PLA fibers, followed by the electro spraying of SiO<sub>2</sub> microparticles (PET/PLA/SiO<sub>2</sub> films). The process was carried out in identical conditions that those applied during electro spinning with the exemption that the SiO<sub>2</sub> solution was pumped at different flow-rates, from 20 to 50 mL/h, through the needle. In addition, for achieving a homogenous electro spraying deposition, the tip-to-collector distance was reduced to 10 cm for the SiO<sub>2</sub> deposition. Once optimization of both jets was achieved, the roll-to roll system worked in a

manner where non-coated PET films went through the injector area for both depositions, continuously moving until reaching the roll collector in which a roll containing coated-PET films was obtained.

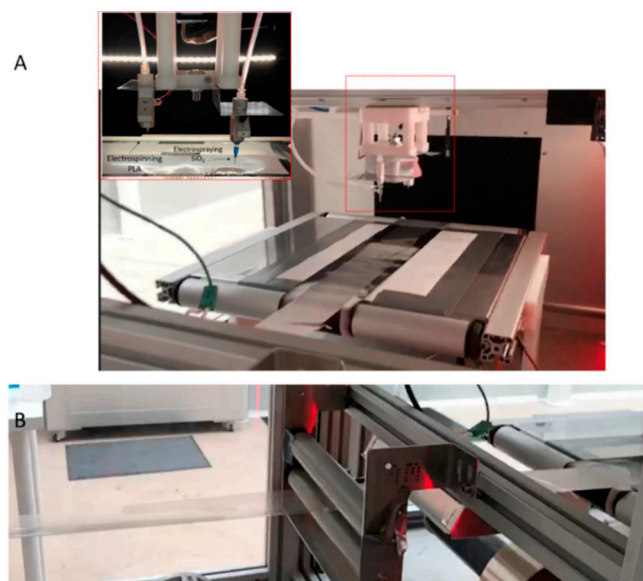


**Figure 1.** (A) Co-continuous electrospinning/electrospraying proprietary setup for the coating of the polyethylene terephthalate (PET) film by polylactide (PLA) fibers and silica ( $\text{SiO}_2$ ) microparticles including an amplified image of the injector. (B) The roll containing the non-coated PET moving continuously from the area of the injector (for the deposition of fibers and microparticles) to the end of the roll collector, where it was collected in a coil-like manner.

### 2.2.3. Thermal Post-Treatment

PET/PLA films and PET/PLA/ $\text{SiO}_2$  films were annealed by placing the PET coated films between Teflon sheets in a hydraulic hot-press model-4122 from Carver, Inc. (Wabash, IN, USA) without applying pressure. Firstly, different temperatures (90 °C, 120 °C, 140 °C, 160 °C, and 170 °C) were applied to the PET/PLA samples in order to find a balance between hydrophobicity, layer adhesion, and film transparency. An annealing time of 15 s was applied to obtain homogenous sample morphology where the structure of the mat was no longer seen. Similarly, for the PET/PLA/ $\text{SiO}_2$  samples, different temperatures (150–170 °C) were applied to optimize interlayer adhesion.

## 2.3. Film Characterization

### 2.3.1. Thickness

The thicknesses of the deposited coatings were measured using an Elektrophysik Minitest 735 from Lumaquin, S.A. (Barcelona, Spain). Four values were measured at various points of the samples after each deposition, that is, PET film, PET/PLA fibers, and PET/PLA fibers/ $\text{SiO}_2$  microparticles. The average and the standard deviation values were determined.

### 2.3.2. Morphology

The morphology of the resulting coatings and multilayer structures were examined by field emission scanning electron microscopy (FESEM) using a Hitachi S-4800 FESEM from Hitachi High Technologies Corp (Tokyo, Japan). An electron beam acceleration of 10 kV and a working distance of 8–10 mm were applied. The materials were sputtered for 3 min with a thin layer of gold/palladium layer prior to FESEM observation. Image analysis was carried out using the Image J Launcher v 1.05 software.

### 2.3.3. Transparency

The absorbance of the films, related to transparency, was determined by UV-Vis spectrophotometry using a UV4000 spectrophotometer from Dinko Instruments (Barcelona, Spain) in a spectral range between 390 and 800 nm. The transparency ( $T$ ) was estimated from the absorption at 600 nm ( $A_{600}$ ) and the thickness of the film in mm ( $L$ ) following the equation  $T = A_{600}/L$  (mm) [23]. For evaluating contact transparency, samples were placed on A4 paper sheets containing letters and imaged.

### 2.3.4. Surface Wettability

The water contact angle ( $\theta$ ) was measured to estimate the wettability of the films with an optical tensiometer in a Video-Based Contact Angle Meter, Theta Lite TL 101 model (Biolin Scientific, Espoo, Finland) using the OneAttension v 3.1 software. A 5- $\mu$ L droplet of distilled water was deposited on the material surface at room temperature and the image of the drop was recorded. Three different measurements were taken and averaged at different parts of the samples. The sliding angle was determined on a water droplet deposited over the surface whilst being tilted and analyzed with the online software Ergonomics Ruler of the Universitat Politècnica de València (UPV), Valencia, Spain (<https://www.ergonautas.upv.es/herramientas/ruler/ruler.php>).

## 3. Results and Discussion

### 3.1. Morphology of Electrospun PLA and Electrosprayed SiO<sub>2</sub> Materials

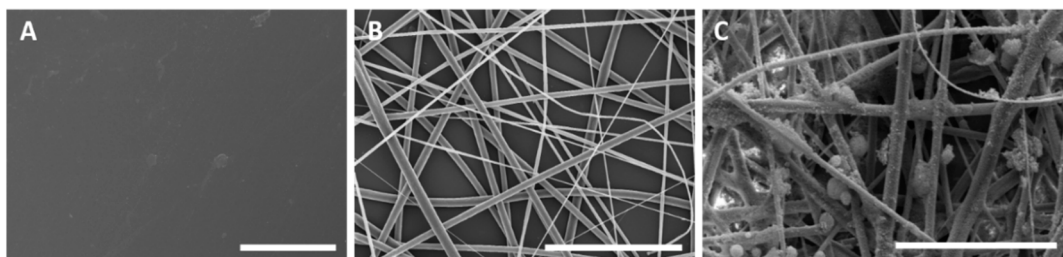
Table 1 includes the mean thickness values of the uncoated PET film and the multilayer films after the deposition of the PLA fibers mat and also the electrosprayed nanostructured SiO<sub>2</sub> microparticles. One can observe that the neat PET film presented a mean thickness of 77  $\mu$ m while the coatings of electrospun PLA fibers and SiO<sub>2</sub> microparticles were approximately 4.2 and 4.6  $\mu$ m, respectively. The thickness was aimed at being the lowest under the screened conditions that could be applied and that could also generate reproducible superhydrophobic and adhesion performance in the final materials.

**Table 1.** Thicknesses of the non-coated polyethylene terephthalate (PET) film and PET films coated by electrospun polylactide (PLA) fibers and electrosprayed silica (SiO<sub>2</sub>) microparticles.

PET	PET/PLA	PET/PLA/SiO <sub>2</sub>
77.0 $\pm$ 0.6 $\mu$ m	81.2 $\pm$ 0.9 $\mu$ m	85.8 $\pm$ 1.3 $\mu$ m

Figure 2 shows the top view of the non-coated and coated PET films. In Figure 2A, one can observe the smooth and continuous surface of the neat PET film. After electrospinning, a mat composed of uniform and randomly oriented PLA fibers with a mean fiber diameter of 1.5  $\pm$  0.7  $\mu$ m was obtained (see Figure 2B). Similar morphologies and sizes have been reported in the literature for PLA fibers obtained under similar electrospinning conditions and solution properties [24]. When SiO<sub>2</sub> microparticles were electrosprayed on the PET/PLA layers, important changes on the surface morphology were observed. Some fibers were coated with SiO<sub>2</sub> nanoparticles (41  $\pm$  6 nm) and also some particles agglomerates (4  $\pm$  0.5  $\mu$ m) were randomly deposited onto the electrospun PLA mat (see Figure 2C). It has been reported that ultrafine particles such as silica nanoparticles tend to agglomerate or aggregate due to the strong cohesive forces between primary particles caused by their high surface-to-volume ratio and the small distance between them [7,25,26].

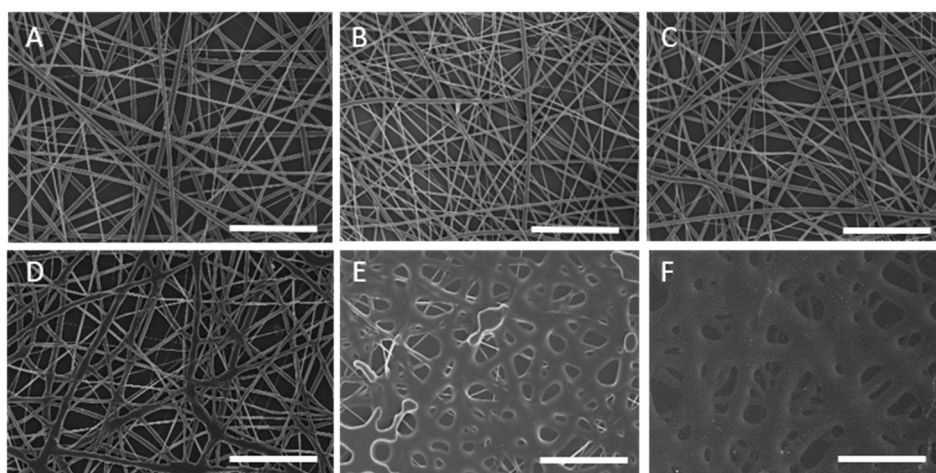




**Figure 2.** (A) Field emission scanning electron microscopy (FESEM) images of the as-received polyethylene terephthalate (PET) film; (B) Electrospun polylactide (PLA) fibers deposited onto the PET film; (C) Electrospayed silica ( $\text{SiO}_2$ ) microparticles onto the PET/PLA fibers. Scale bars of 50  $\mu\text{m}$ .

### 3.2. Characterization of the Electrospun PLA Coated PET Films

The coated PET/PLA fibers were annealed at different temperatures and without pressure, in the range from 90 to 170  $^{\circ}\text{C}$ . Figure 3 shows the top view of the different PET films coated with PLA fibers and annealed at different temperatures. One can observe that, from 140  $^{\circ}\text{C}$  onwards, the PLA fiber morphology was lost due to a process of fibers coalescence. It has been early reported that the thermal post-processing of electrospun fibers well below their melting point leads to a packing of the material into a continuous film with virtually little or no porosity due to fibers coalescence [27,28].



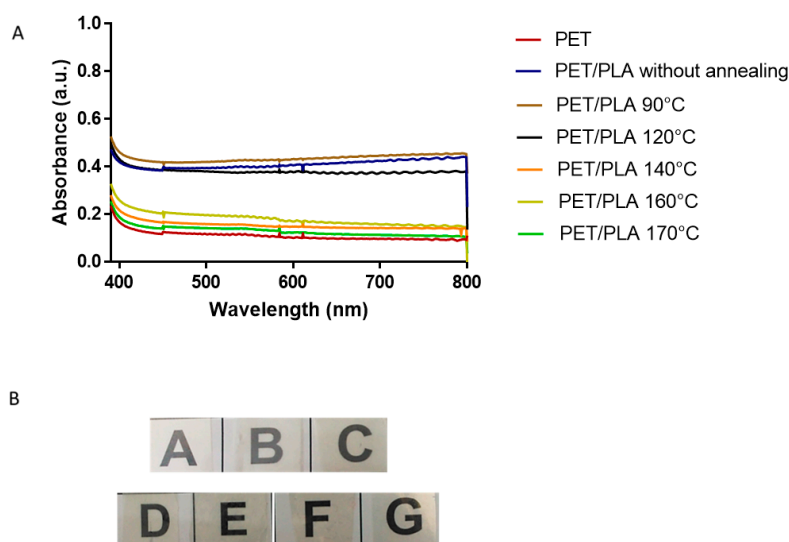
**Figure 3.** Field emission scanning electron microscope (FESEM) micrographs of the polyethylene terephthalate (PET) films coated with electrospun polylactide (PLA) fibers and annealed at different temperatures: (A) Without annealing; (B) 90  $^{\circ}\text{C}$ ; (C) 120  $^{\circ}\text{C}$ ; (D) 140  $^{\circ}\text{C}$ ; (E) 160  $^{\circ}\text{C}$ ; (F) 170  $^{\circ}\text{C}$ . The annealing time was 15 s in all samples and scale bars are 50  $\mu\text{m}$ .

Figure 4 gathers relevant information about the transparency characteristics of the uncoated and coated PET films. Figure 4A shows quantitative measurements of transparency obtained by UV-Vis spectrophotometry in the wavelength range from ca. 400 nm to 800 nm. It can be observed that the uncoated PET film presented a high transparency, with an average light transmittance of 90% in the wavelength range screened. The PLA fibers deposition resulted in a high decrease in transparency to nearly 38% of light transmittance at 600 nm. A similar absorbance was observed for the bilayer structure annealed at 90  $^{\circ}\text{C}$ . The higher absorbance was seen to increase with increasing wavelength. It has been reported that nanofibrous films comprise large amount of air/fiber interfaces and therefore the incident light not only reflects and refracts many times at these interfaces but is absorbed within the mat, resulting in little light being transmitted through [29,30].

An increase in the light transmittance of the bilayer materials were observed when thermal treatments above 120  $^{\circ}\text{C}$  were applied. The sample annealed at 120  $^{\circ}\text{C}$  showed a slight increase in the light transmittance with respect to the non-heated sample. Interestingly, all bilayer structures

annealed at higher temperatures, that is, 140 °C, 160 °C, and 170 °C, presented light transmittance values close to that of the uncoated PET film. Moreover, it was observed that the film transparency was progressively increased as the annealing temperature increased. This behavior was attributed to the fact that these annealing temperatures are closer or just above the first melting feature of the electrospun PLA fibers, previously reported at 154 °C by DSC [22] and in agreement with other previous study [31]. Therefore, it can be stated that the light transmittance of these bilayer films can be significantly enhanced by applying annealing temperatures of at least 140 °C. Similar observations were reported by Cherpinski et al. [28] when carrying out the post-processing optimization of electrospun submicron poly(3-hydroxybutyrate) (PHB) fibers to obtain continuous films.

Figure 4B includes the visual aspect of the film samples to evaluate their contact transparency. It can be observed that contact transparency of the films illustrated a high transparency for PET films and a clear decrease after the PLA fibers were deposited. Interestingly, more transparent films were observed after annealing, especially at temperatures higher than 140 °C. These observations are in expected coherence with the results of the light transmittance studies performed by UV-Vis spectrophotometry mentioned above.



**Figure 4.** (A) Ultraviolet-visible (UV-Vis) transparency measures of the uncoated polyethylene terephthalate (PET) film and coated with electrospun polylactide (PLA) fibers at different annealing temperatures. (B) Contact transparency of the films of: A—Uncoated PET; B—PET/PLA without annealing; C—PET/PLA annealed at 90 °C; D—PET/PLA annealed at 120 °C; E—PET/PLA annealed at 140 °C; F—PET/PLA annealed at 170 °C; and G—PET/PLA annealed at 160 °C. The typical sample size of the films in the pictures is of ca.  $2 \times 1.5 \text{ cm}^2$ .

Figure 5 provides the apparent water contact angle of the PET films coated with electrospun PLA fibers without annealing and annealed at different temperatures. One can observe that the PLA electrospun fibers generated a hydrophobic microdeposition with a value of  $96.17^\circ \pm 10.79^\circ$  that led to a slight increase of water contact angle when compared to the uncoated PET films ( $82.27^\circ \pm 0.83^\circ$ ). This higher contact angle indicates that the water droplet does not spread well on the substrate due to the intrinsic hydrophobicity of the electrospun PLA mats. Contact angles higher than  $120^\circ$  have been reported for PLA, PCL, and poly(lactic-co-glycolic acid) (PLGA) electrospun mats or coatings [8,32].

On the other hand, water contact angles of the PET/PLA films decreased as the temperature of the thermal post-treatment increased, obtaining values of  $83.94^\circ \pm 3.54^\circ$ ,  $80.64^\circ \pm 3.33^\circ$ ,  $79.27^\circ \pm 9.08^\circ$ ,  $75.3^\circ \pm 3.24^\circ$ , and  $73.42^\circ \pm 6.84^\circ$  for the bilayer films treated at 90 °C, 120 °C, 140 °C, 160 °C, and 170 °C, respectively (see Figure 5). In particular, the PET/PLA samples annealed above 140 °C showed a reduction in the contact angles values higher than 20%, in comparison with the coated PET/PLA film without annealing. This effect can be related to the partial loss of the fibrillar roughness structure of the

PLA mat (see Figure 3) and, then, to a reduction of the overall porosity of the film surface, resulting in a decrease of the water contact angle. This behavior is in agreement with the work recently reported by Lasprilla-Botero et al. [8], where LDPE/PCL films were annealed at temperatures ranging from 55 to 90 °C and a loss of surface hydrophobicity was observed as a function of the annealing temperature.

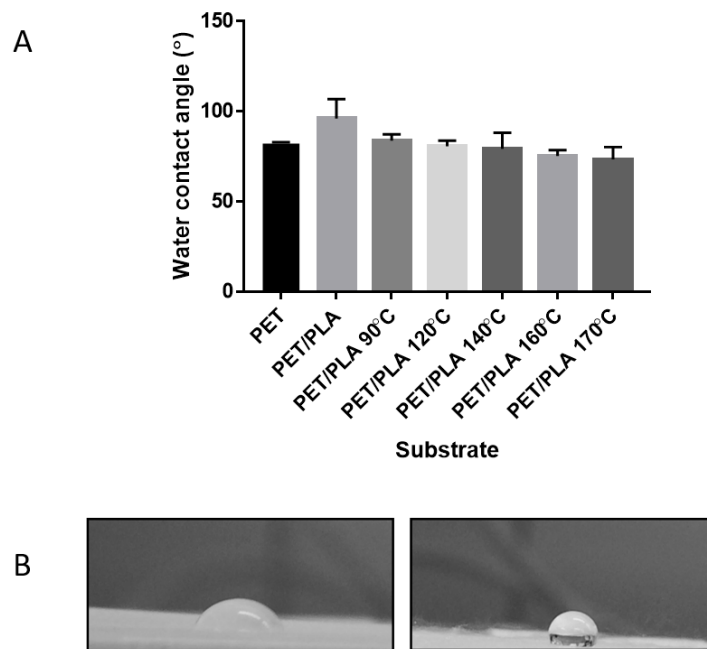


**Figure 5.** (A) Apparent water contact angle measurements of the uncoated polyethylene terephthalate (PET) film and coated with electrospun polylactide (PLA) fibers without annealing and annealed at 90 °C, 120 °C, 140 °C, 160 °C, and 170 °C. The annealing time was 15 s in all samples. (B) Digital images of the contact angle performed on the PET films before (left) and after deposition (right) of the electrospun PLA fibers.

### 3.3. Characterization of the Multilayer PET Films

After optimization of the PLA deposition, achieving superhydrophobicity was attempted by depositing SiO<sub>2</sub> as a second layer on the PET/PLA bilayer structure. For this, different flow-rates were tested during electrospaying, that is, 20 mL/h, 30 mL/h, 40 mL/h, and 50 mL/h and the water contact angle was assessed prior to annealing. Figure 6 shows the values of the contact angle as a function of the flow-rate. One can observe that, after the SiO<sub>2</sub> deposition, superhydrophobicity (>150° on water contact angle) was achieved in all cases, regardless of the flow-rate used.

Since the all tested flow-rates resulted in superhydrophobicity of the multilayer, the lowest flow-rate, that is, 20 mL/h, was chosen for further applying the annealing. It provides higher reproducibility of the application of the SiO<sub>2</sub> microparticles and the optical properties would not be so impaired. Furthermore, superhydrophobicity was already achieved at this flow-rate so there would not be a need to use higher flow-rates, which would have implied a higher production cost in a potential upscaling.

In order to promote adhesion between layers, three different annealing temperatures were chosen, that is, 150 °C, 160 °C, and 170 °C, for the thermal post-treatment in view of the above results on the PET/PLA films. Top and cross-section views of the SEM images of the PET/PLA/SiO<sub>2</sub> films after applying these temperatures are gathered in Figure 7. All the annealing temperatures provoked strong changes in the surface of the multilayer films rendering a rougher topography. The PLA fibers were seen to adhere strongly to the substrate while the SiO<sub>2</sub> microparticles remained well-spread on the PET/PLA bedding substrate.



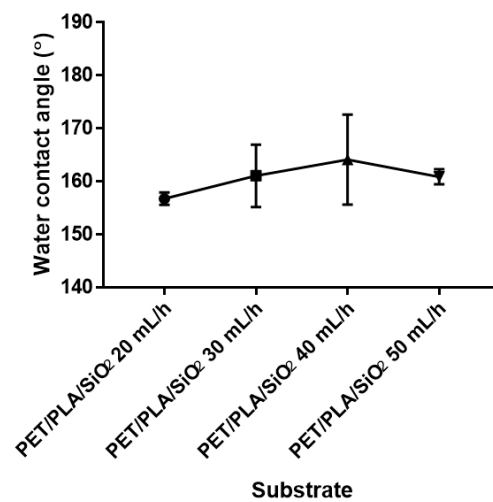


**Figure 6.** Apparent water contact angle of polyethylene terephthalate (PET)/polylactide (PLA)/silica (SiO<sub>2</sub>) films at the electrospinning flow-rates of 20 mL/h, 30 mL/h, 40 mL/h, and 50 mL/h.

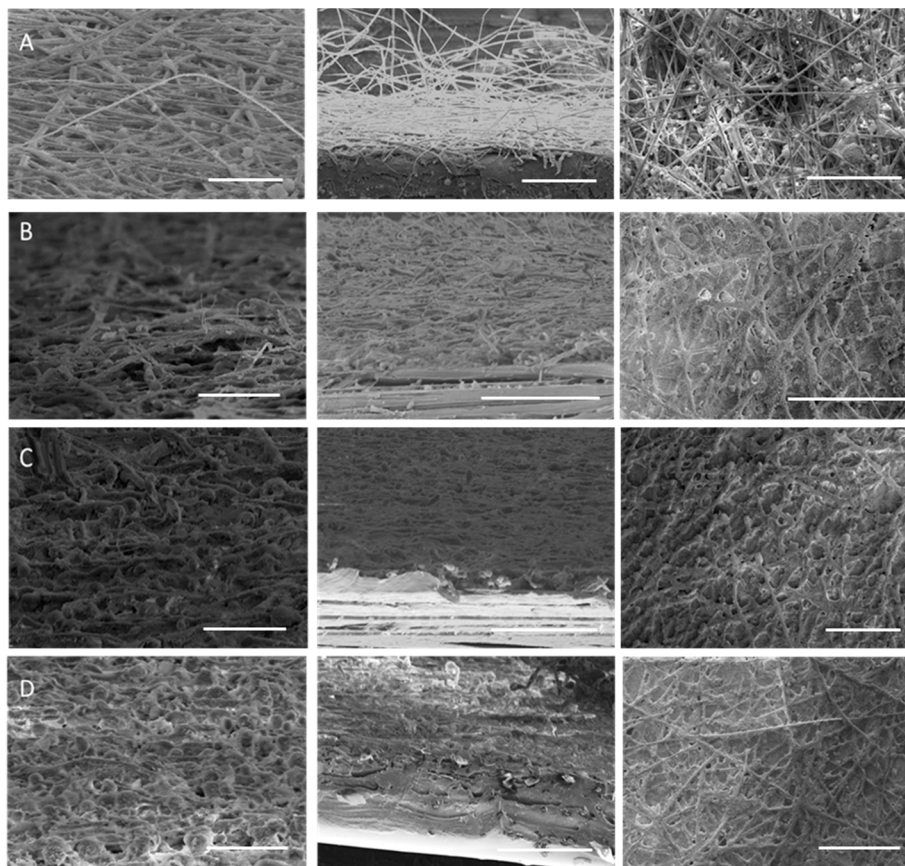


**Figure 7.** Field emission scanning electron microscope (FESEM) micrographs of the cross-section (left and middle columns) and top views (right column) of polyethylene terephthalate (PET)/polylactide (PLA)/silica (SiO<sub>2</sub>) films: (A) Without annealing; (B) Annealed at 150 °C; (C) Annealed at 160 °C; (D) Annealed at 170 °C. The annealing time was 15 s in all samples and scale bars are 50 μm (left column) and 100 μm (middle and right columns).

As one can observe in Figure 8, the thermal treatments applied on the multilayers also resulted in an improvement of the contact transparency when compared with the untreated PET/PLA/SiO<sub>2</sub> film. The transparency values, which take into account the thickness differences among the samples, were, however, similar across the treatments. T values of 6.71, for the treatment at 150 °C, 6.50 for

the treatment at 160 °C, and 5.65 for the highest temperature, that is, of 170 °C, were observed. The T value for the non-treated PET/PLA/SiO<sub>2</sub> was 7.35, while for the uncoated PET it was 1.32 and for the PET/PLA without annealing it was 4.42. In the case of the PET/PLA annealed at 150 °C and 160 °C, the T values were 2.15 and 2.50, respectively. A higher transparency was presented in the PET/PLA samples when comparing the T values with the transparency values of the PET/PLA/SiO<sub>2</sub> films. Likewise, the transmittance light values were lower as compared with the PET/PLA films (see Figure 4), due to the extra layer of sprayed SiO<sub>2</sub> microparticles that diffract the light.

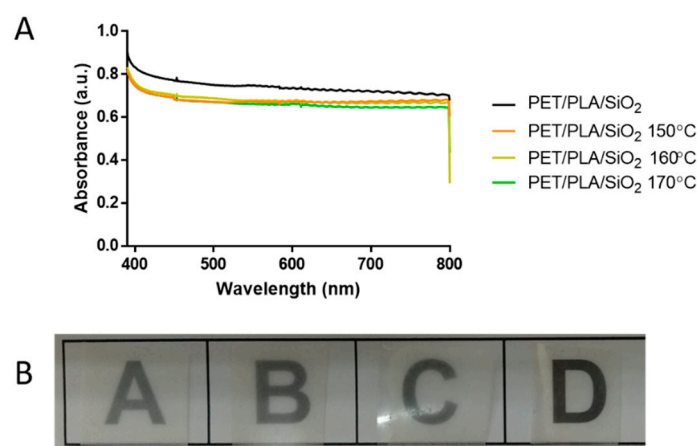


**Figure 8.** (A) Ultraviolet-visible (UV-Vis) transparency measurements of the polyethylene terephthalate (PET)/polylactide (PLA)/silica (SiO<sub>2</sub>) films at different annealing temperatures. (B) Contact transparency of the PET/PLA/SiO<sub>2</sub> films: A—Without annealing; B—Annealed at 150 °C; C—Annealed at 160 °C; D—Annealed at 170 °C. The typical sample size of the films in the pictures is of ca.  $2 \times 1.5 \text{ cm}^2$ .

Lastly, Figure 9 includes the results of the contact angle measurements of the PET/PLA/SiO<sub>2</sub> films. From this figure, it can be observed that all multilayer films rendered a superhydrophobic behavior with contact angle values in the 155°–170° range. The contact angle of the untreated multilayer films was  $156.75^\circ \pm 1.16^\circ$ . Su et al. [7] reported water contact angles around 165° for superhydrophobic structures fabricated via simultaneous electrospinning of SiO<sub>2</sub>/dimethylacetamide (DMAc) colloids and electrospinning of polyvinylidene fluoride (PVDF)/DMAc solutions.

In this context, it was observed that the thermal post-treatment affected the surface superhydrophobicity of the multilayer systems. The film sample annealed at 150 °C showed a low reproducibility in the values of contact angles. It was probably due to the fact that at 150 °C, a partial loss of the fibrillar morphology occurred, provoking a non-homogeneous adherence between layers. When the film samples were treated with the highest temperature, that is, 170 °C, the PLA fibers were completely turned into a continuous film and therefore the contact angle was decreased up to  $158.00^\circ \pm 4.37^\circ$ . The film sample post-treated at 160 °C showed an increase in the contact angle values of around 8%, compared with the untreated multilayer film, obtaining a value of  $170.63^\circ \pm 1.49^\circ$ . Based on these results, it can be stated that thermal post-processing at 160 °C not only improved the adherence between layers but also provided the highest superhydrophobicity. The entrapped air and the roughness structures throughout the depth of the membrane was thought to lead to a continuous water-air-solid interface, resulting in a more hydrophobic surface [7]. In addition, this multilayer material promoted the desired hierarchical nanoparticle-agglomerates-fiber structure (see Figure 7) to increase the tortuosity of the water-air-solid interfaces, thus resulting in an easy sliding, with a sliding angle of 6°.

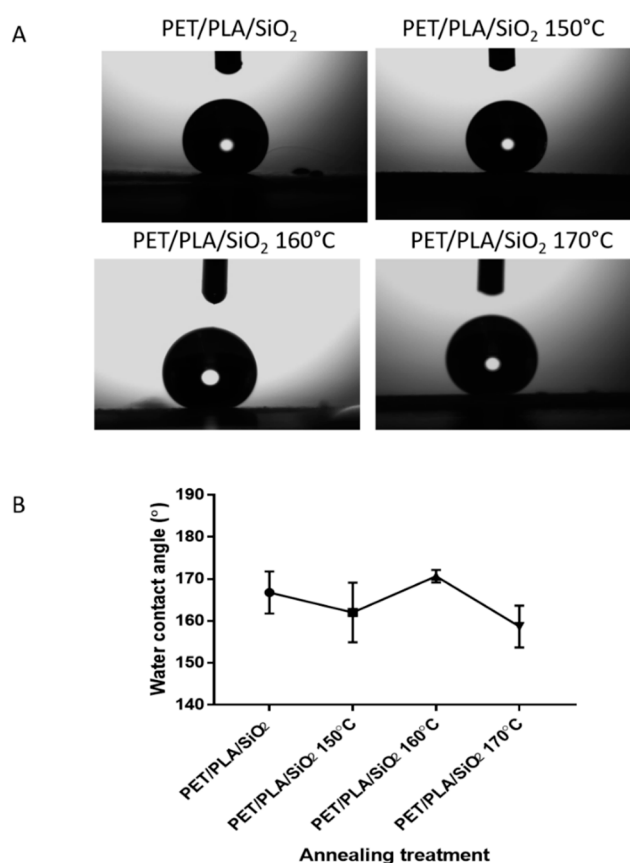


**Figure 9.** (A) Shape of the water droplets on the polyethylene terephthalate (PET)/polylactide (PLA)/silica (SiO<sub>2</sub>) films; (B) Quantitative measurements of the apparent water contact angle of PET/PLA/SiO<sub>2</sub> films without annealing and annealed at 150 °C, 160 °C, and 170 °C.

#### 4. Conclusions

A one-step co-continuous process that can increase the water repellency to PET substrates was herein developed. To this end, first, PLA ultrathin electrospun fibers were deposited onto the PET films by electrospinning and, thereafter, the coated PET/PLA films were post-treated at different annealing temperatures in the 90–170 °C range for 15 s. The control of the solution and electrospinning parameters allowed the creation of a homogeneous deposition of PLA fibers onto the PET films. The presence of the here-developed PLA coatings led to an increase of the surface hydrophobicity of the PET films but did not lead to superhydrophobic properties. For this reason, the co-deposition of SiO<sub>2</sub> microparticles by electrospinning was added to the process. Different electrospinning flow-rates of the SiO<sub>2</sub> microparticles, from 20 to 50 mL/h, generated multilayer films presenting superhydrophobicity. It was observed that the superhydrophobic behavior of the PET/PLA/SiO<sub>2</sub> multilayer films was somewhat improved when thermal post-treatments were applied up to 160 °C. In the optimal formulation, an apparent contact angle of 170° and a sliding angle of 6° were obtained.

Unfortunately, the very high contact and background transparency of PET could not be retained in the double coated samples but after annealing, the optical properties of the coated films with superhydrophobicity were optimal and showed good contact transparency. The generated PET films coated with PLA and SiO<sub>2</sub> reported in this work could be of potential use in easy emptying transparent packaging applications. Furthermore, the reported use of a scaled-up setup with a co-continuous process should facilitate its industrial implementation.

**Author Contributions:** Conceptualization was devised by J.M.L.; Methodology, Validation and Formal Analysis was carried out by M.P.-F., S.T.-G., A.L.-C. and J.M.L. Investigation, Resources, Data Curation, Writing Original Draft Preparation and Writing-Review & Editing was performed by M.P.-F., A.L.-C., S.T.-G. and J.M.L.; Supervision J.M.L.; Project Administration, J.M.L.

**Funding:** This study was funded by the EU H2020 OPTINANOPRO project (No. 686116).

**Acknowledgments:** S.T.-G. would like to thank the Ministry of Science, Innovation, and Universities (MICIU) for his Juan de la Cierva contract (IJCI-2016-29675).

**Conflicts of Interest:** The authors declare no conflict of interest.

## References

1. Bierwagen, G.P. Surface coating. Available online: <https://www.britannica.com/technology/surface-coating> (accessed on 17 September 2018).
2. Maeztu, J.D.; Rivero, P.J.; Berlanga, C.; Bastidas, D.M.; Palacio, J.F.; Rodriguez, R. Effect of graphene oxide and fluorinated polymeric chains incorporated in a multilayered sol-gel nanocoating for the design of corrosion resistant and hydrophobic surfaces. *Appl. Surf. Sci.* **2017**, *419*, 138–149. [[CrossRef](#)]
3. Evstropiev, S.K.; Dukelskii, K.V.; Karavaeva, A.V.; Vasilyev, V.N.; Kolobkova, E.V.; Nikonorov, N.V.; Evstropiyev, K.S. Transparent bactericidal ZnO nanocoatings. *J. Mater. Sci. Mater. Med.* **2017**, *28*, 102. [[CrossRef](#)] [[PubMed](#)]
4. Müller, K.; Bugnicourt, E.; Latorre, M.; Jorda, M.; Echegoyen Sanz, Y.; Lagaron, J.M.; Miesbauer, O.; Bianchin, A.; Hankin, S.; Bölz, U.; et al. Review on the processing and properties of polymer nanocomposites and nanocoatings and their applications in the packaging, automotive and solar energy fields. *Nanomaterials* **2017**, *7*, 74. [[CrossRef](#)] [[PubMed](#)]
5. Suyambulingam, G.R.T.; Jeyasubramanian, K.; Mariappan, V.K.; Veluswamy, P.; Ikeda, H.; Krishnamoorthy, K. Excellent floating and load bearing properties of superhydrophobic ZnO/copper stearate nanocoating. *Chem. Eng. J.* **2017**, *320*, 468–477. [[CrossRef](#)]
6. Barati Darband, G.; Aliofkhaezraei, M.; Khorsand, S.; Sokhanvar, S.; Kaboli, A. Science and engineering of superhydrophobic surfaces: Review of corrosion resistance, chemical and mechanical stability. *Arab. J. Chem.* **2018**. [[CrossRef](#)]
7. Su, C.; Li, Y.; Dai, Y.; Gao, F.; Tang, K.; Cao, H. Fabrication of three-dimensional superhydrophobic membranes with high porosity via simultaneous electrospraying and electrospinning. *Mater. Lett.* **2016**, *170*, 67–71. [[CrossRef](#)]
8. Lasprilla-Botero, J.; Torres-Giner, S.; Pardo-Figueroa, M.; Álvarez-Láinez, M.; Lagaron, J.M. Superhydrophobic bilayer coating based on annealed electrospun ultrathin poly( $\epsilon$ -caprolactone) fibers and electrosprayed nanostructured silica microparticles for easy emptying packaging applications. *Coatings* **2018**, *8*, 173. [[CrossRef](#)]
9. Zhang, X.; Geng, T.; Guo, Y.; Zhang, Z.; Zhang, P. Facile fabrication of stable superhydrophobic SiO<sub>2</sub>/polystyrene coating and separation of liquids with different surface tension. *Chem. Eng. J.* **2013**, *231*, 414–419. [[CrossRef](#)]
10. Nine, M.J.; Cole, M.A.; Johnson, L.; Tran, D.N.H.; Losic, D. Robust superhydrophobic graphene-based composite coatings with self-cleaning and corrosion barrier properties. *ACS Appl. Mater. Interfaces* **2015**, *7*, 28482–28493. [[CrossRef](#)] [[PubMed](#)]
11. Pozzato, A.; Zilio, S.D.; Fois, G.; Vendramin, D.; Mistura, G.; Belotti, M.; Chen, Y.; Natali, M. Superhydrophobic surfaces fabricated by nanoimprint lithography. *Microelectron. Eng.* **2006**, *83*, 884–888. [[CrossRef](#)]
12. Yang, X.; Liu, X.; Lu, Y.; Zhou, S.; Gao, M.; Song, J.; Xu, W. Controlling the adhesion of superhydrophobic surfaces using electrolyte jet machining techniques. *Sci. Rep.* **2016**, *6*, 23985. [[CrossRef](#)] [[PubMed](#)]
13. Hsieh, C.-T.; Chen, W.-Y.; Wu, F.-L. Fabrication and superhydrophobicity of fluorinated carbon fabrics with micro/nanoscaled two-tier roughness. *Carbon* **2008**, *46*, 1218–1224. [[CrossRef](#)]
14. Zhang, Z.; Wang, H.; Liang, Y.; Li, X.; Ren, L.; Cui, Z.; Luo, C. One-step fabrication of robust superhydrophobic and superoleophilic surfaces with self-cleaning and oil/water separation function. *Sci. Rep.* **2018**, *8*, 3869. [[CrossRef](#)] [[PubMed](#)]

15. Hu, C.; Liu, S.; Li, B.; Yang, H.; Fan, C.; Cui, W. Micro-/nanometer rough structure of a superhydrophobic biodegradable coating by electrospraying for initial anti-bioadhesion. *Adv. Healthc. Mater.* **2013**, *2*, 1314–1321. [[CrossRef](#)] [[PubMed](#)]
16. López-Córdoba, A.; Duca, C.; Cimadoro, J.; Goyanes, S. Electrospraying and electrospraying technologies and their potential applications in the food industry. In *Nanotechnology Applications in the Food Industry*; Rai, V.R., Bai, J.A., Eds.; CRC: Boca Raton, FL, USA, 2017.
17. Torres-Giner, S.; Pérez-Masiá, R.; Lagaron, J.M. A review on electrospun polymer nanostructures as advanced bioactive platforms. *Polym. Eng. Sci.* **2016**, *56*, 500–527. [[CrossRef](#)]
18. Torres-Giner, S.; Busolo, M.; Cherpinski, A.; Lagaron, J.M. Electrospraying in the packaging industry. In *Electrospinning: From Basic Research to Commercialization*; Kny, E., Ghosal, K., Thomas, S., Eds.; The Royal Society of Chemistry: London, UK, 2018; pp. 238–260.
19. Torres-Giner, S. Electrospun nanofibers for food packaging applications. In *Multifunctional and Nanoreinforced Polymers for Food Packaging*; Lagaron, J.-M., Ed.; Woodhead Publishing: Cambridge, UK, 2011; pp. 108–125.
20. López-Córdoba, A.; Lagarón, J.M.; Goyanes, S. Fabrication of electrospun and electrosprayed carriers for the delivery of bioactive food ingredients. In *Reference Module in Food Science*; Smithers, G.W., Ed.; Elsevier: Amsterdam, The Netherlands, 2018.
21. Umweltbundesamt Use of Nanomaterials in Coatings. Available online: <https://www.umweltbundesamt.de/en/publikationen/use-of-nanomaterials-in-coatings> (accessed on 17 September 2018).
22. Martínez-Sanz, M.; Lopez-Rubio, A.; Lagaron, J.M. Dispersing bacterial cellulose nanowiskers in polylactides via electrohydrodynamic processing. *J. Polym. Environ.* **2014**, *22*, 27–40. [[CrossRef](#)]
23. Figueroa-Lopez, K.; Castro-Mayorga, J.; Andrade-Mahecha, M.; Cabedo, L.; Lagaron, J. Antibacterial and barrier properties of gelatin coated by electrospun polycaprolactone ultrathin fibers containing black pepper oleoresin of interest in active food biopackaging applications. *Nanomaterials* **2018**, *8*, 199. [[CrossRef](#)] [[PubMed](#)]
24. Casasola, R.; Thomas, N.L.; Trybala, A.; Georgiadou, S. Electrospun poly lactic acid (PLA) fibres: Effect of different solvent systems on fibre morphology and diameter. *Polymer* **2014**, *55*, 4728–4737. [[CrossRef](#)]
25. Syed, J.A.; Tang, S.; Meng, X. Super-hydrophobic multilayer coatings with layer number tuned swapping in surface wettability and redox catalytic anti-corrosion application. *Sci. Rep.* **2017**, *7*, 4403. [[CrossRef](#)] [[PubMed](#)]
26. Yao, W.; Guangsheng, G.; Fei, W.; Jun, W. Fluidization and agglomerate structure of SiO<sub>2</sub> nanoparticles. *Powder Technol.* **2002**, *124*, 152–159. [[CrossRef](#)]
27. Cherpinski, A.; Torres-Giner, S.; Cabedo, L.; Méndez Jose, A.; Lagaron, J.M. Multilayer structures based on annealed electrospun biopolymer coatings of interest in water and aroma barrier fiber-based food packaging applications. *J. Appl. Polym. Sci.* **2017**, *135*, 45501. [[CrossRef](#)]
28. Cherpinski, A.; Torres-Giner, S.; Cabedo, L.; Lagaron, J.M. Post-processing optimization of electrospun submicron poly (3-hydroxybutyrate) fibers to obtain continuous films of interest in food packaging applications. *Food Addit. Contam. Part A* **2017**, *34*, 1817–1830. [[CrossRef](#)] [[PubMed](#)]
29. Cherpinski, A.; Gozutok, M.; Sasmazel, H.; Torres-Giner, S.; Lagaron, J. Electrospun oxygen scavenging films of poly (3-hydroxybutyrate) containing palladium nanoparticles for active packaging applications. *Nanomaterials* **2018**, *8*, 469. [[CrossRef](#)] [[PubMed](#)]
30. Tang, C.; Liu, H. Cellulose nanofiber reinforced poly (vinyl alcohol) composite film with high visible light transmittance. *Compos. Part A Appl. Sci. Manuf.* **2008**, *39*, 1638–1643. [[CrossRef](#)]
31. Garlotta, D. A literature review of poly (lactic acid). *J. Polym. Environ.* **2001**, *9*, 63–84. [[CrossRef](#)]
32. Russo, V.; Tammaro, L.; Di Marcantonio, L.; Sorrentino, A.; Ancora, M.; Valbonetti, L.; Turriani, M.; Martelli, A.; Cammà, C.; Barboni, B. Amniotic epithelial stem cell biocompatibility for electrospun poly (lactide-co-glycolide), poly ( $\epsilon$ -caprolactone), poly (lactic acid) scaffolds. *Mater. Sci. Eng. C* **2016**, *69*, 321–329. [[CrossRef](#)] [[PubMed](#)]

